Quantitative Analysis of Rate-Dependent of Human Heart Failure Action Potential Model on Alternans Onset and Arrhythmias

M. M. Elshrif[1], P. Shi[1], E. M. Cherry[2]

[1] B. Thomas Golisano College of Computing and Information Sciences, Rochester Institute of Technology, Rochester, USA
[2] School of Mathematical Sciences, Rochester Institute of Technology, Rochester, USA

Abstract

It is known that at the living organism level, heart failure (HF) increases the susceptibility to and incidence of cardiac alternans, both of which are strongly associated with sudden cardiac death (SCD). We use mathematical models to investigate how electrophysiological properties consistent with heart failure affect the onset and magnitude of electrical alternans and its mechanism compared to similar cases in normal human cells. We study how APD restitution curves and short-term memory are altered in normal and HF-affected cells and tissue. We compare our results with available experimental observations and find good agreement.

1. Introduction

Cellular alternans, which is a beat-to-beat alternation in action potential duration (APD) is closely associated with ventricular arrhythmias and SCD experimentally [1] and clinically [2]. APD alternans may arise from the dynamics of one or more of ionic currents or from intracellular calcium dynamics.

Previous research on alternans during heart failure focused on analyzing the relationship between T-wave alternans and SCD. For example, [3] found that patients with systolic dysfunction are at risk for VT/VF based on the presence and magnitude of T-wave alternans. Also, [4] speculates that T-wave alternans may caused by a steep APD restitution curve, which may lead to APD alternans and could progress to VT/VF ultimately at rapid pacing rates [5]. However, some evidence suggests that T-wave alternans arises from the cellular level [6]. However, studies of alternans in human ventricular models to date have focused on examining the alternans under normal settings [7, 8]. It is important to investigate alternans dynamics under HF conditions to help elucidate the reasons for increased susceptibility to arrhythmias under HF conditions.

In this paper, we study alternans under HF conditions and compare its dynamics with normal cells and tissue. In particular, we analyze APD restitution curves, effects of pacing history and the influence of cellular coupling alternans dynamics under both conditions [9].

2. Methods

To investigate alternans under normal and HF conditions, we conduct computer simulations of isolated single cells and one-dimensional cable domains of cardiac tissue using the epicardial, midmyocardial, and endocardial cell type of the O'Hara et al. (OVVR) original model [8] and the HF-modified HF O'Hara et al. model [10]. Both models can be described in a single cell by the following differential equation:

$$\partial_t V_m = -(1/C_m)(I_{ion} + I_{stim}), \quad (1)$$

where V_m is the transmembrane potential, C_m is the membrane capacitance, I_{ion} is the sum of all transmembrane currents, and I_{stim} is the stimulus current.

In a one dimensional cable, we solved the following monodomain representation of cardiac tissue:

$$\partial_t V_m = -(1/C_m)(I_{ion} + I_{stim}) + D\partial_x^2 V_m, \quad (2)$$

where D is the diffusion constant.

In all cases, initial conditions were obtained by pacing at a cycle length (CL) of 1000 ms with applied current strength twice diastolic threshold until the difference between two successive action potentials (APs) was on the order of 10^{-4} ms.

Both models were implemented with a time resolution of 0.02 ms using an explicit Euler method and a spatial resolution of 0.015 cm. The calcium equations were integrated with a finer time step of 0.001 ms.

APDs were measured using the voltage threshold corresponding to 90% repolarization after pacing for 30 s at a CL of 1000 ms. APD alternans was considered to be present when variations in APD between consecutive beats

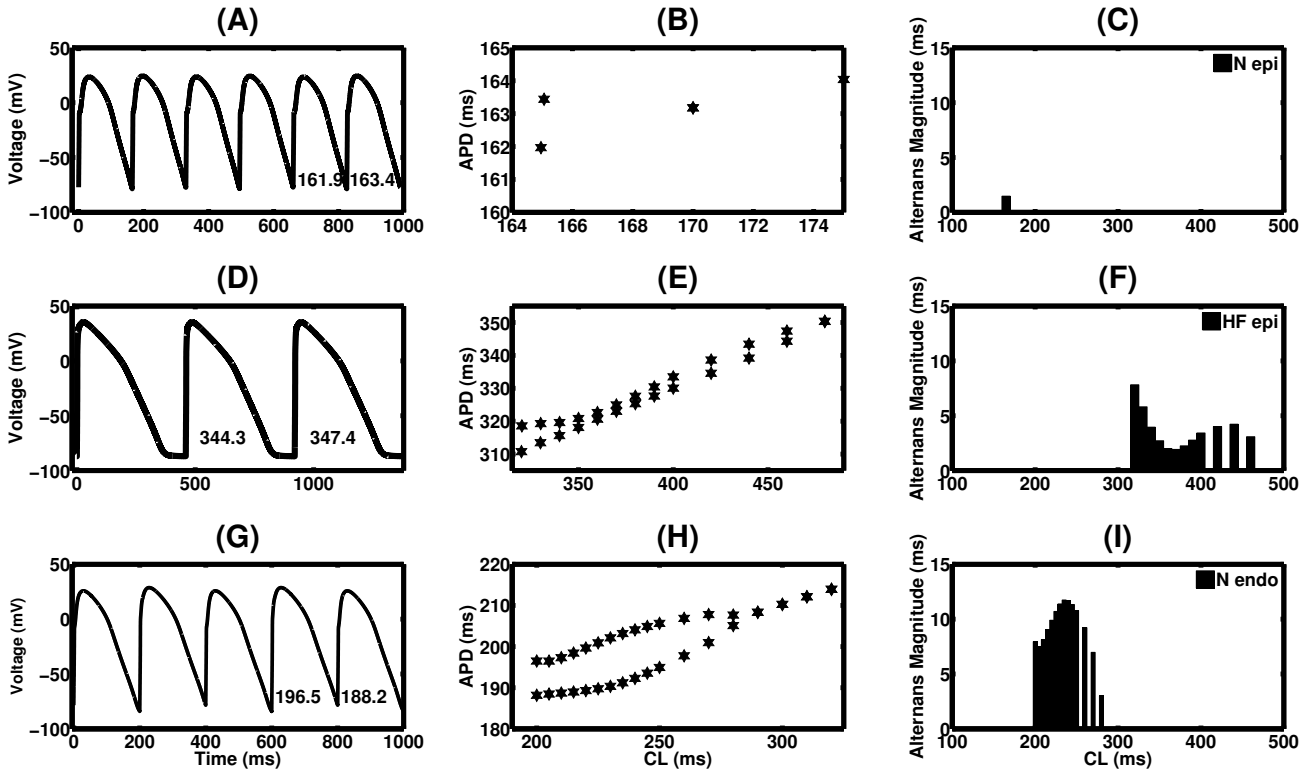

Figure 1. Alternans in a single cell (0D). (A) APs of non-failing (N) epicardial cells. (B) Corresponding bifurcation diagram of the non-failing epicardial cell. (C) Alternans magnitude distribution of the non-failing epicardial cell. (D) APs of failing epicardial cells. (E) Corresponding bifurcation diagram of the failing epicardial cell. (F) Alternans magnitude distribution of the failing epicardial cell. (G) APs of non-failing endocardial cells. (H) Corresponding bifurcation diagram of the non-failing endocardial cell. (I) The alternans magnitude distribution of the non-failing endocardial cell.

is 1.5 ms. For the 1D case, the stimulation current was applied to one edge of the cable. The measurement of beat-to-beat APD alternans was taken from the central cell of the cable to be isolated from edge effects. The 1D cable was composed of 100 cells. The alternans magnitude is measured as the unsigned difference of the APDs of two consecutive beats at steady state.

To investigate the effects of the slopes of restitution curves on the onset and dynamics of alternans, we measured the slopes of steady-state (S-S) and S1-S2 restitution curves. For the S-S protocol, the cell was stimulated for 30 s starting at a CL of 1 s after which the CL was decreased monotonically until 2:1 block was observed. At each CL, the last APD and the prior diastolic interval (DI) pair were registered (during alternans, the last two DI, APD pairs were recorded). For the S1-S2 protocol, the cell was stimulated for 30 s with a fixed CL, represented as S1, after which a subsequent stimulation (S2) was applied after a variable DI. The last values for DI and APD were measured. The memory amplitude was calculated as the difference in APD for the longest DI between the longest S1 CL (here, 1 s), and the shortest S1 CL before conduction block or alternans was observed [9].

3. Results

Figure 1 shows alternans properties observed in single cells. For single epicardial cells, we found that the onset of alternans occurs at a higher CL in HF cells, 460.0 ms, compared with normal cells, 165.0 ms. Also, the range of alternans cycle lengths in HF cells is extended to 320.0-460.0 ms, compared with normal cells, 165.0 ms. We observed that HF cells possess larger alternans magnitude, 8.0 ms, compared with normal cells, which possess 1.5 ms. Thus, alternans is obtained more easily under HF conditions.

For endocardial single cells, we observe that the alternans onset for normal cells is 280.0 ms, with a wide range of CLs showing alternans between 280.0 ms and 200.0 ms. Also, the alternans magnitude between 3.0 ms and 12.0 ms. Under HF conditions, we did not observe any alternans. Instead, the cell reached 2:1 block without displaying alternans.

For midmyocardial single cells, we did not observe alternans under either normal or HF conditions; instead, the

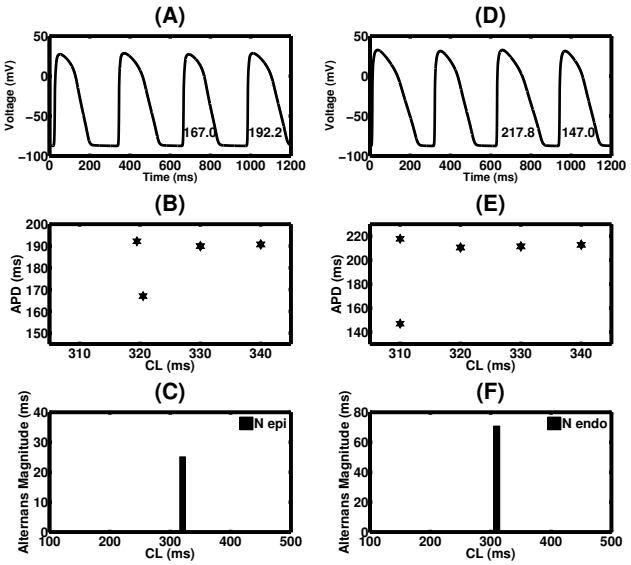

Figure 2. Alternans in a one dimensional cable (1D). (A) APs of non-failing epicardial cells. (B) Bifurcation diagram of the non-failing epicardial cable. (C) Alternans magnitude distribution of the non-failing epicardial cable. (D) APs of non-failing endocardial cells. (E) Bifurcation diagram of the non-failing endocardial cable. (F) Alternans magnitude distribution of the non-failing endocardial cable.

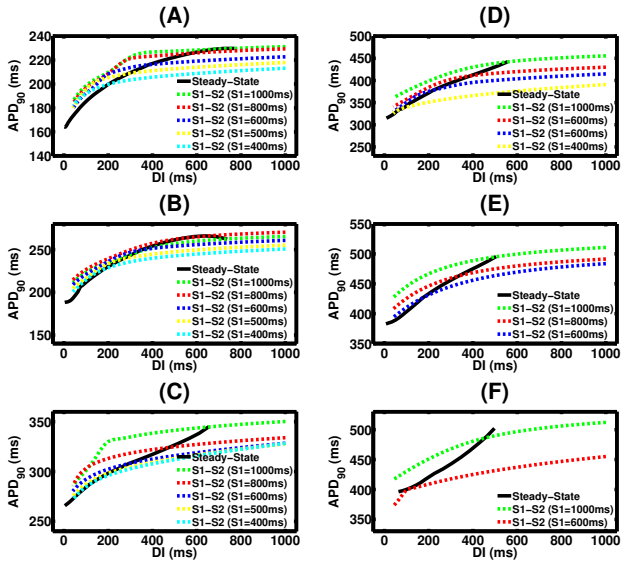

Figure 3. Steady-state (S-S) and S1-S2 APD restitution curves in a single cell. (A) Non-failing epicardial cell. (B) Non-failing midmyocardial cell. (C) Non-failing endocardial cell. (D) Failing epicardial cell. (E) Failing midmyocardial cell. (F) Failing endocardial cell.

cells were unable to fully repolarize and got blocked.

As shown in Fig. 2, in a 1D cable, the alternans onset occurred at a CL of 320.0 ms for epicardial cells under normal conditions and lasted for only one cycle length. However, the alternans magnitude was 25.1 ms. Similar behavior was observed for endocardial cells under normal conditions, where the alternans onset occurred at a CL of 310.0 ms for only that one CL. However, the alternans magnitude was very large at 70.8 ms. We did not observe any alternans in cables composed of midmyocardial cell under either condition or for epicardial and endocardial cells under HF conditions.

As can be seen in Fig. 3, for single cells, the maximum slopes of the S-S restitution curves increase slightly in HF conditions for both epicardial (HF: 0.5, normal: 0.4) and midmyocardial (HF: 0.4, normal: 0.2) cells. However, for the endocardial cell type, the slope of the S-S restitution curve decreased (HF: 0.3, normal: 0.7). In tissue, both epicardial and midmyocardial myocytes showed steeper slopes for the S-S restitution curves (epi HF: 0.2, normal: 0.1; mid HF: 0.5, normal: 0.2), but the slope did not change from endocardial myocytes to cables, with the maximum slope being 0.2, as can be seen in Fig. 4.

For single cells, the maximum slopes of the S1-S2 restitution curves for all types of cells increased slightly under heart failure conditions (epi HF: 0.4, normal: 0.3; mid HF: 0.5, normal: 0.4; endo HF: 0.3, normal: 0.2); see Fig. 3. In tissue, we observed mixed results, as shown in Fig. 4.

4. Discussion and Conclusion

For single epicardial cells, we found that the onset of alternans was increased in HF cells to 460.0 ms, compared with the onset in normal cells at 165.0 ms. Also, the range of alternans cycle lengths in HF cells increased to 320.0-460.0 ms, compared with the value in normal cells of 165.0 ms, which is close to the measured value in experiments CL$\leq$240 ms for control and CL$\leq$500 ms for HF in tissue. This finding is in agreement with data that normal human ventricles do not exhibit electrical alternans at slow rates [11, 12].

In addition, the range of alternans magnitudes in epicardial single cells, 2.0-8.0 ms, overlaps with the range that has been observed in an ischemic cardiomyopathy patient of 3.0$\pm$1.0 ms [13].

The onset CL of alternans increased in a 1D cable in both cases, normal and HF. Also, 2:1 block was reached in 1D cables at larger CLs than in 0D cells. Alternans occurs in the normal OVVR model in tissue for a single CL of 320 ms in epicardial cells and a single CL of 310 ms in endocardial cells; the magnitudes of alternans for those cell types were 25.2 and 70.8 ms, respectively. [14] found the alternans onset occurred at a much lower CL of 267 ms, with a maximum alternans magnitude of 11.0 ms. Thus, although alternans occurs for the normal OVVR model, it

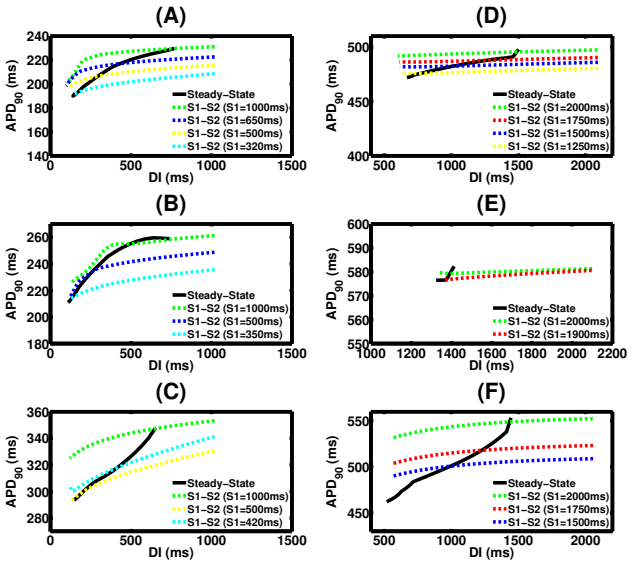

Figure 4. Steady-state (S-S) and S1-S2 APD restitution curves in 1D cables. (A) Non-failing epicardial cable. (B) Non-failing midmyocardial cable. (C) Non-failing endocardial cable. (D) Failing epicardial cable. (E) Failing midmyocardial cable. (F) Failing endocardial cable.

present earlier and achieves a significantly greater magnitude than what has been observed clinically.

Our model includes some limitations. Recent work on mRNA [15] has shown that alternans in human HF cells begins at a CL of 350 ms, whereas alternans in our case begins at a CL 110 ms higher, but our model includes this CL in the alternans range, which is 460.0-320.0 ms. In addition, this onset value closer to the observed values reported in other studies [16] where the alternans occurred for CLs $\leq$500 ms.

We have found that our simulations in single cells and 1D cables are capable of producing alternans that are in agreement with experimental observations on control and HF.

Acknowledgements

This work has been financially supported by the Libyan-North American Scholarship Program from the Ministry of Higher Education, Scientific Research in Libya, the Ph.D. Program in Computing and Information Sciences at RIT, and the National Science Foundation under Grant Number CMMI-1028261.

References

[1] Weiss JN, Karma A, Shiferaw Y, Chen P, Garfinkel A, Qu Z. From pulsus to pulseless: The saga of cardiac alternans. Circulation Research 2006;98(10):1244–1253.

[2] Surawicz B, Fisch C. Cardiac alternans: diverse mechanisms and clinical manifestations. J Am Coll Cardiol 1992; 20(2):483–99.

[3] Narayan MS. T-wave altemans and the susceptibility to ventricular arrhythmias. J Am Coll Card 2006;47(2):269–281.

[4] Weiss JN, Karma A, Shiferaw Y, Chen PS, Garfinkel A, Qu Z. From pulses to pulseless: the saga of cardiac alternans. Circ Res 2006;98(10):1244–53.

[5] Koller MLea. Altered dynamics of action potential restitution and altemans in humans with structural heart disease. Circulation 2005;12(11):1542–48.

[6] Pastore JMea. Mechanism linking t-wave alternans to the genesis of cardiac fibrillation. Circulation 1999; 99(10):1385–1394.

[7] Elshrif MM, Cherry EM. A quantitative comparison of the behavior of human ventricular cardiac electrophysiology models in tissue. PLoS ONE 2014;9:e84401.

[8] O'Hara T, Virag L, Varro A, Rudy Y. Simulation of the undiseased human cardiac ventricular action potential: Model formulation and experimental validation. PLoS Comput Biol 2011;7(5):e1002061.

[9] Cherry EM, Fenton FH. A tale of two dogs: analyzing two models of canine ventricular electrophysiology. American Journal of Physiology Heart and Circulatory Physiology 2007;292(1):H43–H55.

[10] Elshrif M, Shi P, Cherry E. Electrophysiological properties under heart failure conditions in a human ventricular cell: A modeling study. The IEEE EMBC 2014;.

[11] Narayan MSea. T-wave altemans, restitution of human action potential duration, and outcome. J Am Coll Cardiol 2007;50(25):2385–92.

[12] Ashihara T, Yao T, Ito M, et al. Steep apd restitution curve is not essential for microvolt t-wave alternans: insights from computer simulations (abstr). Heart Rhythm 2007;4:S92.

[13] Narayan MS, Bayer JD, Lalani G, Trayanova NA. Action potential dynamics explain arrhythmic vulnerability in human heart failure: a clinical and modeling study implicating abnormal calcium handling. J Am Coll Cardiol 2008; 52(22):1782–92.

[14] Myerburg RJ, Castellanos A. Emerging paradigms of the epidemiology and demographics of sudden cardiac arrest. Heart Rhythm 2006;3(2):235–239.

[15] Walmsley J, Rodriguez JF, Mirams GR, Burrage K, Efimov IR, Rodriguez B. mrna expression levels in failing human hearts predict cellular electrophysiological remodeling: A population-based simulation study. PLoS ONE 2013;8(2):e56359.

[16] Wilson LD, Jeyaraj D, Wan X, Hoeker GS, Said TH, Gittinger M, Laurita KR, Rosenbaum DS. Heart failure enhances susceptibility to arrhythmogenic cardiac alternans. Heart Rhythm 2009;6(2):251 – 259.

Address for correspondence:

Mohamed Elshrif
Bldg 74, Room 1065, 102 Lomb Memorial Drive,
Rochester, NY 14623, USA
mme4362@rit.edu